2006

Vascular Morphometry of the Retina in Antarctic Fishes is Dependent upon the Level of Hemoglobin in Circulation

Jody M. Wujcik

VASCULAR MORPHOMETRY OF THE RETINA IN ANTARCTIC FISHES IS DEPENDENT UPON THE LEVEL OF HEMOGLOBIN IN CIRCULATION

By

Jody M. Wujcik

B.S. East Stroudsburg University, 2004

A THESIS

Submitted in Partial Fulfillment of the

Requirements for the Degree of

Master of Science

(in Marine Biology)

The Graduate School

The University of Maine

August, 2006

Advisory Committee:

Bruce D. Sidell, Professor of Marine Sciences, Advisor

Harold B. Dowse, Professor of Biological Sciences

Seth Tyler, Professor of Zoology and Cooperating Professor of Marine Sciences

VASCULAR MORPHOMETRY OF THE RETINA IN ANTARCTIC FISHES IS DEPENDENT UPON THE LEVEL OF HEMOGLOBIN IN CIRCULATION

By Jody M. Wujcik

Thesis Advisor: Dr. Bruce D. Sidell

An Abstract of the Thesis Presented
in Partial Fulfillment of the Requirements for the
Degree of Master of Science
(in Marine Biology)
August, 2006

Antarctic notothenioids express the circulating oxygen-binding protein hemoglobin (Hb) over a broad range of blood concentrations. White-blooded icefishes (Suborder: Notothenioidei, Family: Channichthyidae) are the only known adult vertebrates to lack Hb completely. In addition to its role in oxygen transport, Hb is the primary reactant in degradation of nitric oxide (NO). Thus, NO should be degraded at a slower rate in Hb-lacking icefishes than in Hb-expressing notothenioids, leading to higher steady-state levels of NO in the former group. Increased levels of NO should stimulate upregulation of angiogenesis, the growth and proliferation of new blood vessels from existing vasculature. Based upon these relationships, our laboratory proposes that an inverse correlation exists between vascular density and Hb concentration. Morphometric parameters of retinal vascular anatomy of Antarctic fishes with varying hematocrit (Hct) were quantified and the relationship between vascular density and Hct was assessed. Retinal tissue is particularly amenable to quantification because the entire vascular array is essentially a two-dimensional sheet, eliminating the need for three-dimensional

reconstructions. Digital images of retinal vessels filled with a silicone rubber compound (Microfil^{TM}) were analyzed using a macro for MATLAB 7.1 developed for this study. Icefishes display mean blood vessel length densities (*Chaenocephalus aceratus*, 5.51±0.32 mm/mm^2; *Champsocephalus gunnari*, 5.15±0.50 mm/mm^2) that are greater than those observed in red-blooded species (*Gymnodraco acuticeps*, 5.20±0.46 mm/mm^2; *Parachaenichthyes charcoti*, 4.40±0.30 mm/mm^2). Hemoglobinless (-Hb) fishes have average vessel diameters that are ~1.5 times larger than vessel diameters of +Hb species (-Hb, 0.193±0.006 mm; +Hb, 0.125±0.005 mm). The combination of greater length densities and larger diameter vessels results in fractional image areas (i.e., vessel surface areas) that are greater in –Hb icefishes (*C. aceratus*, 49.1±2.23%; *C. gunnari*, 43.8±3.6%) than those seen in +Hb fishes (*G. acuticeps*, 33.0±4.1%; *P. charcoti*, 23.8±1.0%). Vascular density index (VDI), a stereological indicator of vessel number and length, is greatest in -Hb *C. aceratus* (3.51±0.20) and lowest in +Hb *Notothenia coriiceps* (1.58±0.14). Among four species of +Hb fishes with a >2.3-fold range of Hct, retinal VDI is inversely correlated with Hct (R^2=0.934) and intervessel distance in retinal tissue is positively correlated with Hct (R^2=0.898). Within this group of closely related fishes, vascular capacity to supply blood to the retina increases as Hct decreases. The direct relationship between VDI and Hct is consistent with the hypothesis of NO-mediated angiogenesis.

ACKNOWLEDGEMENTS

With sincere gratitude, I thank my advisor, Dr. Bruce Sidell, for his endless support and guidance during this academic endeavor. I also thank the other members of my advisory committee, Dr. Dusty Dowse and Dr. Seth Tyler, for their input over the past two years. I want to acknowledge our collaborators, Dr. Joe Eastman of Ohio University and George Wang of the University of Washington, for their key contributions to this research. Great appreciation goes out to Kelly Edwards of The University of Maine EM Lab for his help in the early stages of this project. Thanks to Kim Borley, a great labmate and friend, and also to the residents of Murray Hall and the SMS community for making my time at U. Maine a truly pleasant experience. In addition, I am thankful to the masters and crew of the ARSV *Laurence M. Gould* and the support personnel of Raytheon Polar Services for contributing to a safe and enjoyable field season in Antarctica. This research was supported by NSF Grants OPP 01-25890 and ANT 04-37887 to B.D.S.

On a more personal note, I gratefully acknowledge the help and encouragement of my family. I specifically want to thank my mother and mother-in-law for their assistance while I was away conducting field research. I am also thankful to my mom for her love and support throughout all of my academic years of study. Most importantly, I want to thank my husband, Jason, and my two children, Jessica and Lukas, for their patience and understanding during the never-ending times that I was lost in my work. Finally, with heartfelt gratitude, I want to acknowledge my father by dedicating this to him.

TABLE OF CONTENTS

LIST OF TABLES

LIST OF FIGURES

Chapter 1

Introduction

The Southern Ocean, including waters from the Antarctic continent to the Antarctic Polar Front, encompasses over 35 million square kilometers, approximately 10% of the world's ocean (Laws, 1985). It is the coldest, densest, and most thermally stable marine habitat on the planet. Continental shelf waters continuously hover at or below -1.86°C, the freezing point of seawater, and throughout most of the Southern Ocean, from the surface to great depths, temperatures vary as little as 4-5°C (Knox, 1970; Lewis and Perkin, 1985). Cold temperatures do have a benefit. Because gas solubility is inversely proportional to temperature, oxygen content in Antarctic waters is extremely high. These conditions preclude organisms from experiencing environmental hypoxia under normal circumstances (Littlepage, 1965). Unlike the constancy of temperature, photoperiod is highly variable. In McMurdo Sound for instance, biota are faced with a four-month period of continual darkness in winter and perpetual light in summer. During two-month transition periods, photoperiod increases or decreases by as much as 20 minutes per day (Rivkin and Putt, 1987). In addition to seasonal effects, downwelling irradiance is further attenuated by presence of snow, ice, and sea ice microbial communities (Sullivan et al., 1984).

In spite of harsh environmental conditions, there is one group of animals that has flourished in the Southern Ocean. Fishes of the perciform suborder Notothenioidei dominate the fish fauna of waters south of the Antarctic Polar Front. Consisting of 8 families, 43 genera, and 122 species, notothenioids comprise approximately 35% of fish

species and 90% of fish biomass in the region (Eastman and Eakin, 2000). Over the last few decades notothenioids have provided scientists with many insights about the physiological and biochemical adaptations to cold body temperatures.

Notothenioids occupy a variety of habitat niches; some species are benthic or epibenthic, while others are pelagic, semipelagic or cryopelagic (Gon and Heemstra, 1990). Activity levels vary among species from sedentary to active. In red-blooded fishes, behavioral activities are related to concentrations of the circulating oxygen-binding protein, hemoglobin (Hb). Not surprisingly, Hb content and number of erythrocytes are higher in more active species (Wells et al., 1980). Nototheniids of the ecologically diverse Family Nototheniidae have relatively high and variable Hb contents, whereas dragonfishes, members of the Family Bathydraconidae, possess lower levels of Hb (Eastman, 1993).

Antarctic icefishes, Family Channichthyidae, are the only known vertebrate animals to lack Hb completely as adults (Ruud, 1954). In the absence of Hb, oxygen is carried strictly in physical solution in the blood. This results in an oxygen carrying capacity in icefishes that is <10% of that seen in red-blooded notothenioids (Holeton, 1970). Modifications of the cardiovascular system compensate for the loss of this important respiratory protein. Icefishes possess large-bore capillaries and have blood volumes that are ~2-4 times larger than those of red-blooded fishes (Fitch et al., 1984; Hemmingsen and Douglas, 1970). Additionally, hearts are larger in icefishes than in similar-sized red-blooded fishes, resulting in weight-specific cardiac outputs that are several-fold greater than those of red-blooded species (Hemmingsen et al., 1972; Holeton, 1970). Integration of these features allows channichthyids to circulate large

blood volumes at relatively high flow rates. This is achieved at low aortic blood pressures due to decreased systemic flow resistance. Ultimately, the combination of high throughput cardiovascular systems, high oxygen content waters, and low absolute metabolic rates enables this group of fishes to deliver sufficient oxygen to their tissues (Hemmingsen, 1991).

In addition to enhanced cardiovascular systems, channichthyids display another noteworthy feature. Vasculature associated with the retina of the eye is exceptionally dense in -Hb fishes compared to that in +Hb species (Eastman, 1988; Eastman and Lannoo, 2004; Sidell and O'Brien, 2006). These vessels, located at the vitreoretinal interface, are properly termed hyaloid arteries because unlike true retinal arteries, they do not travel within the retina (Walls, 1942). Hence, like most lower vertebrates, the retina of notothenioids is considered avascular (Chase, 1982). Derived from the internal carotid artery, the hyaloid artery enters the sclerad surface of the retina within the optic nerve and, at the optic disc, divides into a branching network of vessels on the vitrad surface of the retina. Hyaloid arteries then drain to a circumferential receiving vessel, the annular vein, located medial to the ora serrata (Eastman, 1988). Close spacing of hyaloid vessels in channichthyids effectively reduces the diffusion distance for oxygen, thus ensuring greater oxygenation of the underlying retina. This is highly beneficial to fishes that are already compromised by a reduction in oxygen-carrying capacity brought about by loss of Hb.

Most physiological work to date on notothenioids has focused on questions pertaining to respiratory and cardiovascular function related to reduced or complete absence of Hb. However, recent research suggests that another important role for Hb

may have been overlooked. In addition to binding oxygen, Hb is the primary reactant in degradation of nitric oxide (NO) to nitrate (Gardner, 2005). NO is a small, uncharged, and highly diffusible molecule that mediates a broad array of biological functions (Kerwin et al., 1995). NO is one of the products of a 5-electron oxidation of L-arginine and oxygen catalyzed by the enzyme nitric oxide synthase (NOS). There are three distinct forms of NOS: endothelial NOS (eNOS, NOS-III), neuronal NOS (nNOS, NOS-I), and inducible NOS (iNOS, NOS-II) (Moncada and Higgs, 1993). eNOS and nNOS are constitutively expressed in mammals, whereas iNOS is stimulated by factors such as cytokines and hypoxia (Kerwin et al., 1995). Over the past few years, presence of each of these isoforms has been documented in teleosts (Fritsche et al., 2000; Holmqvist et al., 2004; Tota et al., 2005).

Nitric oxide is involved in a number of physiological processes including neurotransmission, cardiovascular regulation, immunological reactions, and inflammatory responses (Kerwin et al., 1995; Moncada, 1997). The most well known role for NO is perhaps that of a vasodilator (Palmer et al., 1987). However, NO is also implicated in angiogenesis, the growth and proliferation of new blood vessels from preexisting vasculature. Angiogenesis occurs through two mechanisms; sprouting of new vessels from the sides and ends of existing vessels or by longitudinal splitting of existing vessels (Conway et al., 2001). NO also induces upregulation of vascular endothelial growth factor (VEGF), a key promoter in blood vessel proliferation (Kimura et al., 2000). VEGF, in concert with Angiopoietin-1, facilitates enlargement of lumenal diameters of blood vessels (Suri et al., 1998). Recent research also has indicated that NO plays a role

in hypoxia- and exercise-induced angiogenesis in muscle (Kimura et al., 2000; Milkiewicz et al., 2005).

Given the relationships between Hb and nitric oxide, our laboratory hypothesizes that NO degradation should occur at a slower rate in -Hb channichthyids than in +Hb notothenioids, leading to higher steady-state levels of NO in the former group. Consequently, increased levels of NO should stimulate upregulation of angiogenesis and enhanced vascular densities will be observed. Based upon that projection, an inverse correlation should exist between vascular density and Hb concentration. Indeed, preliminary evidence bears this out. Qualitative accounts clearly indicate that vascular densities in retinal tissues are greatest in -Hb channichthyids and intermediate to low in +Hb notothenioids with different Hb contents. To investigate these associations further, objectives of this study included: (1) a quantitative characterization of morphometric parameters of retinal vasculature in Antarctic notothenioids with varying levels of Hb and (2) an assessment of the relationship between vascular density and Hb concentration.

Chapter 2

Materials and methods

Animals

Six species of notothenioid fishes were collected from aboard the ARSV *Laurence M. Gould* in the austral autumn (April-May) of 2005 from waters of the Antarctic Peninsula region. *Chaenocephalus aceratus*, *Champsocephalus gunnari*, *Gymnodraco acuticeps*, *Parachaenichthyes charcoti,* and *Notothenia coriiceps* were primarily caught by otter trawl at 85-200 m depth near Astrolabe Needle (64° 08'S, 62° 40'W) in Dallman Bay. *Trematomus hansoni* was captured in baited benthic pot traps at 250-500 m depth from either the Neumayer Channel (64° 30'S, 62° 34'W) or Palmer Basin (64° 50'S, 64° 04'W). Animals were kept in circulating seawater tanks and transported to the U.S. Antarctic Research Station, Palmer Station on Anvers Island, where they were maintained unfed, in covered aquaria containing circulating seawater at -0.8 ± 0.3 °C.

Tissue preparation

To visualize vascular features, blood vessels of fishes were filled with Microfil™ (Flow Tech, Inc.), a liquid silicon rubber compound. Animals were first anesthetized with MS-222 in seawater (1:7,500 w/v) for a period of 10-15 minutes. Next, a 0.3-1.0 ml dose (specimen size dependent) of concentrated heparinized notothenioid Ringer solution (2500 U/ml heparin added to 260 mM NaCl, 2.5 mM $MgCl_2 \cdot 6\ H_2O$, 5.0 mM KCl, 2.5 mM $NaHCO_3$, 5.0 mM $NaH_2PO_4 \cdot H_2O$, pH 8.0) was injected into the caudal vein and the

animal was promptly returned to a holding bucket for an additional 10 minutes. Fishes were then placed ventral side up on an iced surgical platform and a series of incisions were made to open the pericardial cavity. The heart (atrium and ventricle) was removed, leaving the bulbus arteriosus intact *in situ*. The bulbus arteriosus was cannulated with PE-tubing (90, 100, 160, or 190) and ligated with surgical silk. The cannula was then connected to tubing leading to a B-D syringe (10, 20, or 30 ml) loaded in a KD Scientific Model 100 syringe pump. Approximately 15-30 ml of ice-cold heparinized notothenioid Ringer solution (760 U/ml heparin added to 260 mM NaCl, 2.5 mM $MgCl_2 \cdot 6\ H_2O$, 5.0 mM KCl, 2.5 mM $NaHCO_3$, 5.0 mM $NaH_2PO_4 \cdot H_2O$, pH 8.0) was perfused throughout the entire vascular system at a flow rate of ≤46.8 ml/hr. Specimens were then filled with 9-27 ml of ice-cold yellow Microfil™ using the same apparatus at a flow rate of ≤34.2 ml/hr. While allowing the Microfil™ to polymerize, specimens were maintained on ice for about one hour, followed by a one-week fixation in 10% formalin and subsequent storage in 70% ethanol.

After initial anesthetization and prior to the injection of concentrated heparinized ringer solution, a blood sample was taken from each red-blooded individual for determination of hematocrit. Blood was drawn from the caudal vein using a 20.5 gauge needle, transferred into two heparanized hematocrit capillary tubes, and then centrifuged for ~5 minutes in a hematocrit microcentrifuge (LW Scientific). Using digital calipers, hematocrit was calculated as the percent of packed red blood cells in the total volume of blood.

Fixed specimens were transported back to our home laboratory at the University of Maine where eyes were excised from each specimen as part of an intact, rectangular

block of tissue, approximately 1.5 × 2.0 inches in dimension. To visualize the hyaloid vessels at the vitreoretinal interface, the sclera, cornea, iris, and lens were cut away anterior to the margin of the ora serrata. The vitreous body was carefully extracted from the vitreous chamber by a combination of discrete cutting with iridectomy scissors and subsequent removal with blunt nosed forceps.

Photography

Digital images were taken using a Nikon D70 camera fitted with a 60 mm AF Micro Nikkor lens and mounted on a stand approximately 27-28 inches above the plane of the vessels. Images were shot in aperture mode (F51) to compensate for the large depth of field of the eye. Additionally, camera settings were as follows: optimize image, vivid; image quality, fine; image size, large; white balance, incandescent; ISO-200. Light sources included a Fiber-Lite MI-150 Illuminator (Dolan-Jenner Industries) centered directly below the lens of the camera and two incandescent spotlights positioned on the sides at 45° angles. During the photographic procedure, eyes were secured in a shallow Petri dish and covered with 70% ethanol. Several photographs were taken of each eye, including photos with a scale bar. The best image of the series was chosen for further processing.

Image processing

Original digital images were processed using ImageJ (Version 1.32 from NIH) on a Sony VAIO personal notebook computer (Figure 2.1, A). Images were cropped using the oval region of interest tool (ROI). The oval ROI was centered over the optic disc and

extended outward until point of contact with the margin of the eye, forming an oval-shaped reference field containing the majority (>90%) of the hyaloid vessels present at the vitreoretinal interface (Fig. 2.1, B). Next, an RGB color split was performed to isolate the yellow, the optimum channel for viewing the vessels. An edge finder, FJ Laplacian plugin with a derivative smoothing scale of 3, was used on the yellow channel image to maximize detection of the vessels from the background. The image was enhanced in a series of steps starting with conversion to 8-bit, inversion, and automatic adjustment of brightness and contrast. For further optimization, another separation of channels was performed by "subtracting" the blue from the current "Result of Laplacian" image, followed by automatic adjustment of brightness and contrast again. The resultant image was then converted to binary via the threshold function (Fig. 2.1, C). For a few of the images, there were discrete areas where vessels obviously did not fill with Microfil™. These regions were cropped from the reference field. As a processing control, vessel diameters from the binary image were compared to vessel diameters of the original image. Differences between the two never exceeded 5%.

Procedure for inadequately filled specimens

Two species did not fill successfully with Microfil™. A successful vascular fill was considered to be one where ≥90% of the blood vessels on the vitrad surface of the retina was filled with Microfil™. *Trematomus hansoni* and *Notothenia coriiceps* did not meet this criterion; therefore an alternative method was devised to demonstrate the ocular vasculature of these species. Tissues were stained with a solution of 1% aniline blue in saturated picric acid for approximate 1-2 minute duration. After rinsing with distilled

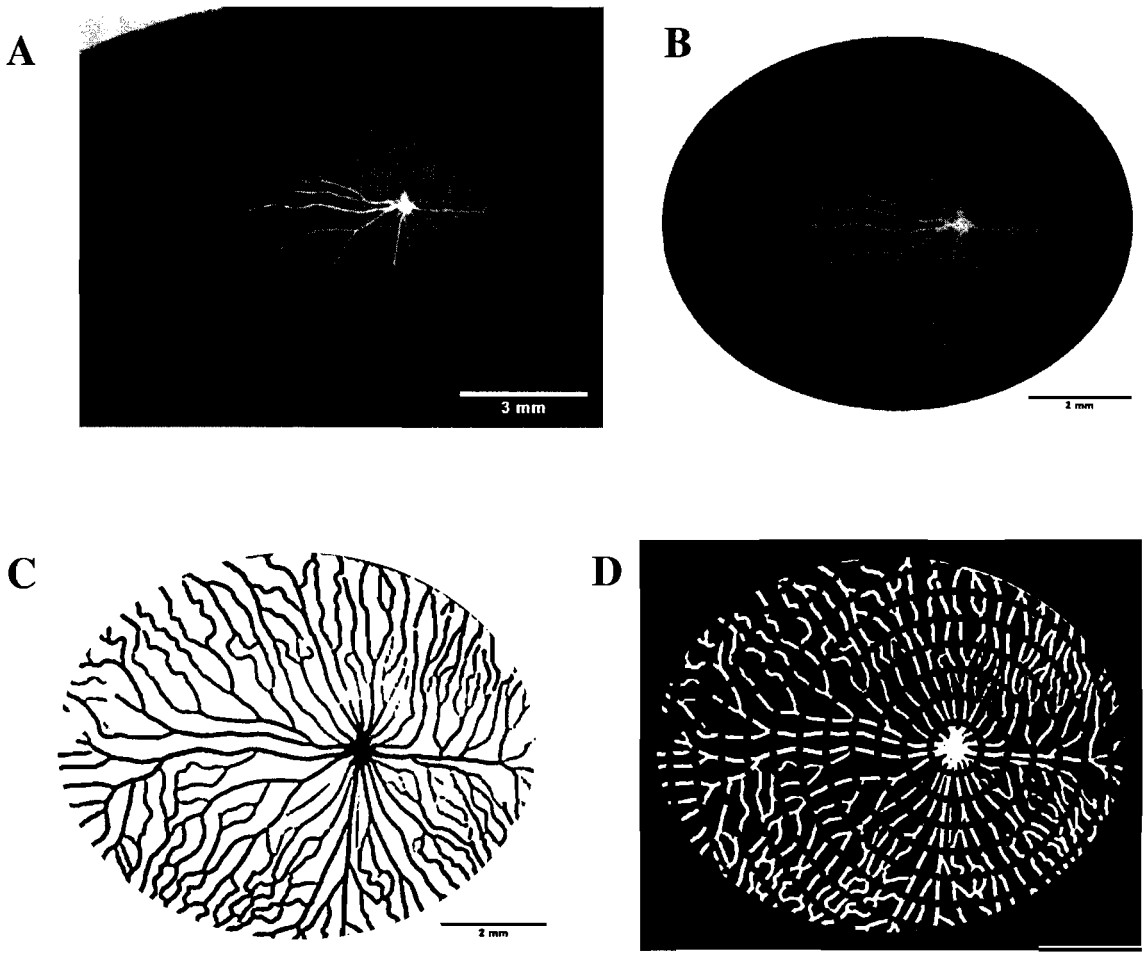

Figure 2.1. Representative digital images of the hyaloid arteries on the vitrad surface of the retina of *Parachaenichthyes charcoti*, a red-blooded bathydraconid. (A) Original digital image; (B) cropped image; (C) binary image; (D) binary image with superimposed concentric circle overlay. The green and red markings denote vessels included in morphometric analyses. Scale bar = 3 mm for image A and scale bars = 2 mm for images B, C, and D.

water, each eye was dissected further and returned to 70% ethanol. Blood vessels were then discernable and further removal of the vitreous body was possible with less concern for possible destruction of previously obscured vessels. For most of the specimens, staining and subsequent dissection had to be repeated several times before the tissue was in satisfactory condition to be photographed.

Digital images of the stained eyes were taken as previously described. Using Adobe Photoshop (7.0) each image was converted to grayscale and contrast was adjusted to give maximal differentiation between the vessels and background. A transparent layer was superimposed on top of the grayscale image and blood vessels were traced using a digitizing tablet (DrawingBoard III, GTCO CalComp Inc.), while simultaneously verifying the actual vessels under a dissecting microscope. The brightness and contrast of the digitized drawing were adjusted so that the grayscale background layer disappeared (turned white) and the vessel layer (already black) remained, thus completing the conversion of the image to binary.

Image analysis

Morphometric measurements of retinal vascularity were obtained using an automated macro (developed by George Wang, University of Washington) in MATLAB (7.1). The design of the macro was based on previous studies analyzing angiogenic response (Maas et al., 1999; Strick et al., 1991). A concentric circle overlay was superimposed on each computerized binary image with the first circle centered directly over the optic disc (Fig. 2.1, D). The diameter of the innermost circle was 1.0 mm and spacing between successive circles was fixed at 0.5 mm. Vascular density index (VDI), a

stereological indicator of blood vessel length and number, was computed by dividing the number of vessel-grid intersections by the total circumference of the circles within the reference field. The VDI was first calculated for the entire reference field, the whole eye. Each image was entered into MATLAB twice and the average of the counts was recorded as the mean VDI for that specimen. The difference between the two counts was used to assess intra-observer variability. To examine vascular density as a function of distance from the optic disc, the VDI for each individual gridline was recorded. The reference field was divided into four quadrants (QI-ventrotemporal; QII-dorsotemporal; QIII-dorsonasal; QIV- ventronasal), with the optic disc as the point of origin, to analyze VDI as a function of location within the fundus.

In addition to VDI, several other morphometric measurements were obtained using the MATLAB macro. Individual vessel diameters, measured to the outside wall, were recorded at each vessel-grid intersection, averaged together and reported as a mean for the entire eye. The intervessel distance (IVD) for each gridline was calculated by dividing the circumference of the circle by the number of intersecting vessels. Once again, calculations were averaged for the whole eye and IVD was reported as a mean. Length density, the total length of vessels per unit area, was derived using the principle of Buffon by multiplying VDI by $\pi/2$ (Weibel 1979). Data were collected for one other morphometric parameter; ImageJ was used to measure fractional image area, the percent of reference field covered by blood vessels. Fractional image areas were calculated for entire eyes and quadrants.

Statistical analyses

Comparisons among the six species for each morphometric measurement were performed in SigmaStat (3.1) using a One-Way ANOVA with a *post-hoc* Student-Newman-Keuls test for multiple pairwise comparisons of the means. The alpha value was set at $P \leq 0.05$. Linear least squares regression was used to analyze the relationship between hematocrits and the following: vascular densities, intervessel distances, specimen total lengths, and specimen body masses. Additionally, intra-observer variability associated with operation of the MATLAB macro was assessed. Variability was calculated by dividing the standard deviation of the paired differences between replicates by the overall mean VDI.

Chapter 3

Results

Hematocrits and vascular patterns

Hematocrits (Hct) ranged from 16.1% in *G. acuticeps* to 37.5% in *N. coriiceps*, an approximate 2.3-fold difference among four species of red-blooded notothenioids, (Table 3.1). Within species, Hct did not appear to be related to body size (correlation coefficient $R^2<0.50$ for all species). Vascular densities and branching patterns in retinal tissues vary in relation to Hct. The greatest vascular densities and most complex branching patterns are seen in hemoglobinless (-Hb) fishes (Figure 3.1). *C. aceratus* displays a branching pattern where four or five vessels exit the optic disc and divide into an anastomosing array of closely spaced parallel channels on the fundus of the eye. *C. gunnari* exhibits a radial distribution of four or five main vessels originating from the optic disc and branching in a dichotomous pattern. Vascular densities in red-blooded (+Hb) bathydraconids (*G. acuticeps*, *P. charcoti*) appear less dense than vessel densities in icefishes, but have similar radial branching patterns to that of *C. gunnari* (Figure 3.2). Vessel densities exhibited by *T. hansoni* (+Hb notothenid) are comparable to the densities of bathydraconids, particularly *P. charcoti* (Figure 3.3). Vessels in *N. coriiceps*, another +Hb notothenid, are very sparse and represent a vascular density pattern that completely contrasts that of *C. aceratus* (Fig. 3.3).

Table 3.1. Hematocrits and physical characteristics of Antarctic notothenioid fishes

	Channichthyidae		Bathydraconidae		Nototheniidae	
	Chaenocephalus aceratus (-Hb)	*Champsocephalus gunnari* (-Hb)	*Gymnodraco acuticeps* (+Hb)	*Parachaenichthyes charcoti* (+Hb)	*Trematomus hansoni* (+Hb)	*Notothenia coriiceps* (+Hb)
Hematocrit (%)	X	X	16.1 ± 6.0	26.1 ± 2.7	24.4 ± 6.4	37.5 ± 1.1*
Body Mass Range (g)	175 - 931	397 - 477	154 - 241	66 - 491	186 - 583	437 - 719
Total Length Range (cm)	33 - 51	39 - 42	30 - 34	25 - 42	25 - 36	33 - 37

X denotes lack of hemoglobin; hematocrit not determined.
Hematocrit values are means ± S.E.M.; N=2 for *G. acuticeps*; N=5 for *P. charcoti*; N=3 for *T. hansoni*; N=4 for *N. coriiceps*.
* denotes that *N. coriiceps* has a significantly greater hematocrit than *G. acuticeps*.

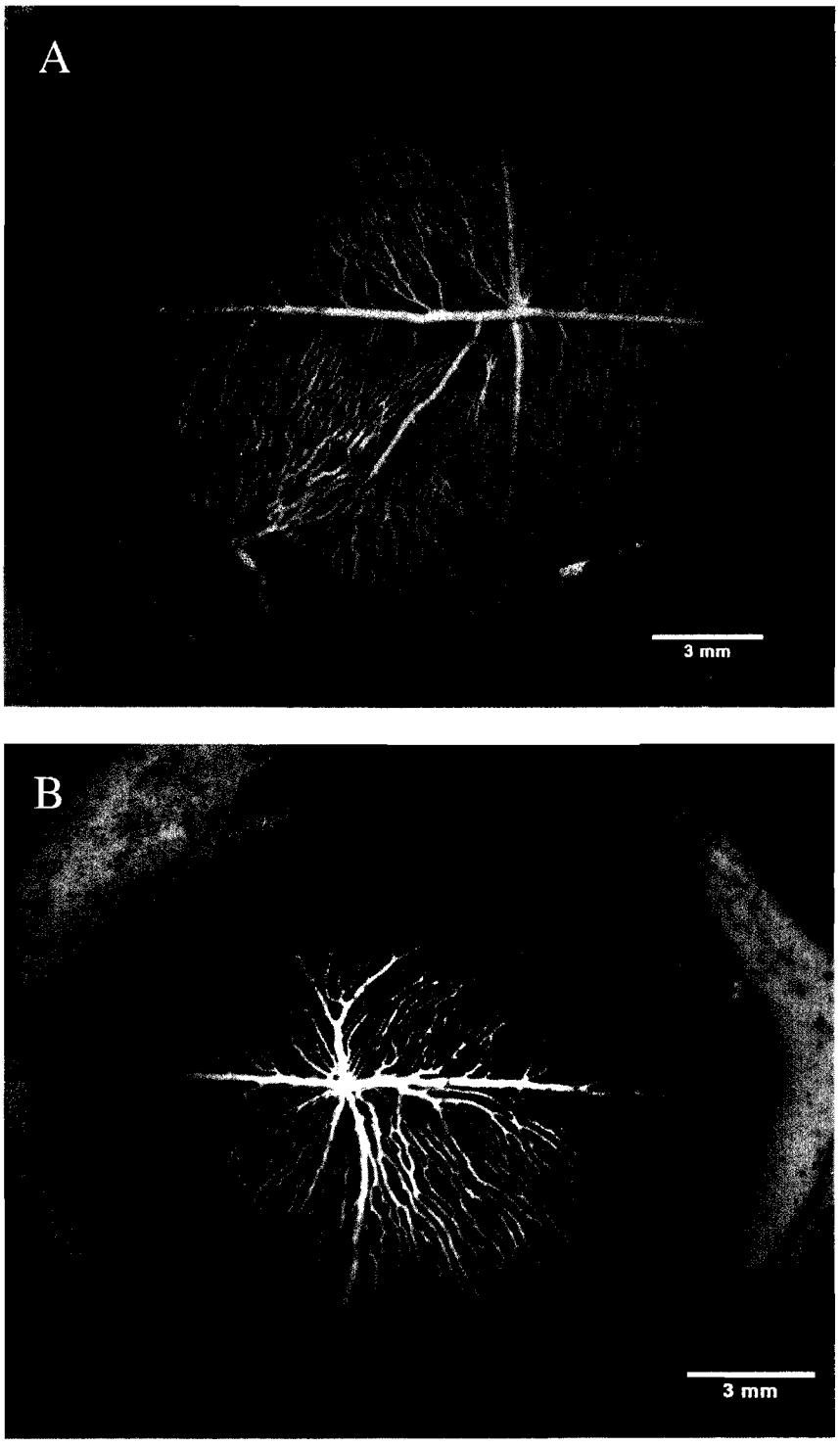

Figure 3.1. Representative digital images of the hyaloid vessels on the vitrad surface of the retina of two species of Channichthyid fishes (-Hb). (A) *Chaenocephalus aceratus*; (B) *Champsocephalus gunnari*. The cornea, iris, lens, and vitreous body were removed to allow viewing of the hyaloid vasculature. Blood vessels were filled with yellow Microfil™.

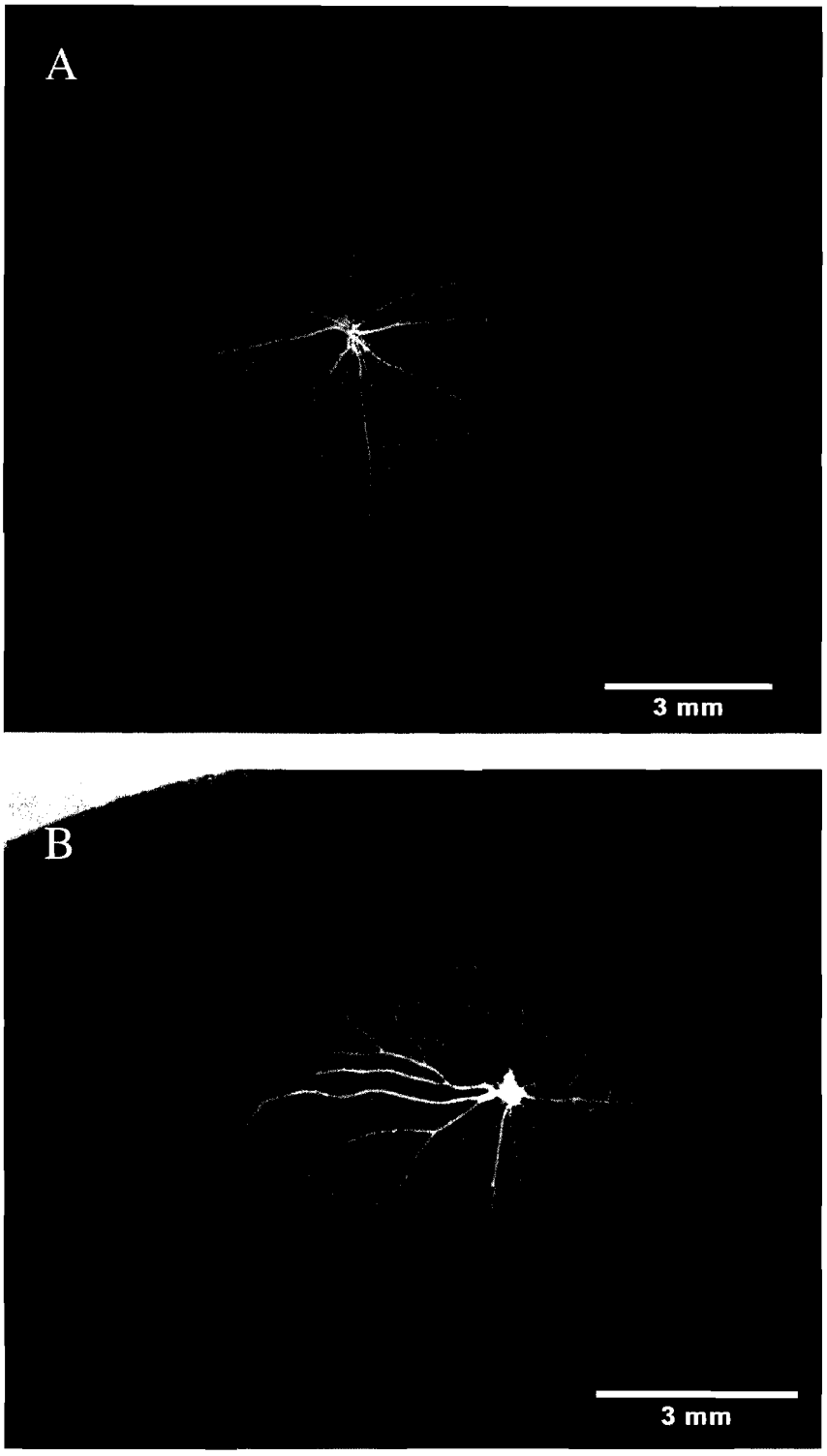

Figure 3.2. Representative digital images of the hyaloid vessels on the vitrad surface of the retina of two species of Bathydraconid fishes (+Hb). (A) *Gymnodraco acuticeps*; (B) *Parachaenichthyes charcoti*. The cornea, iris, lens, and vitreous body were removed to allow viewing of the hyaloid vasculature. Blood vessels were filled with yellow Microfil™.

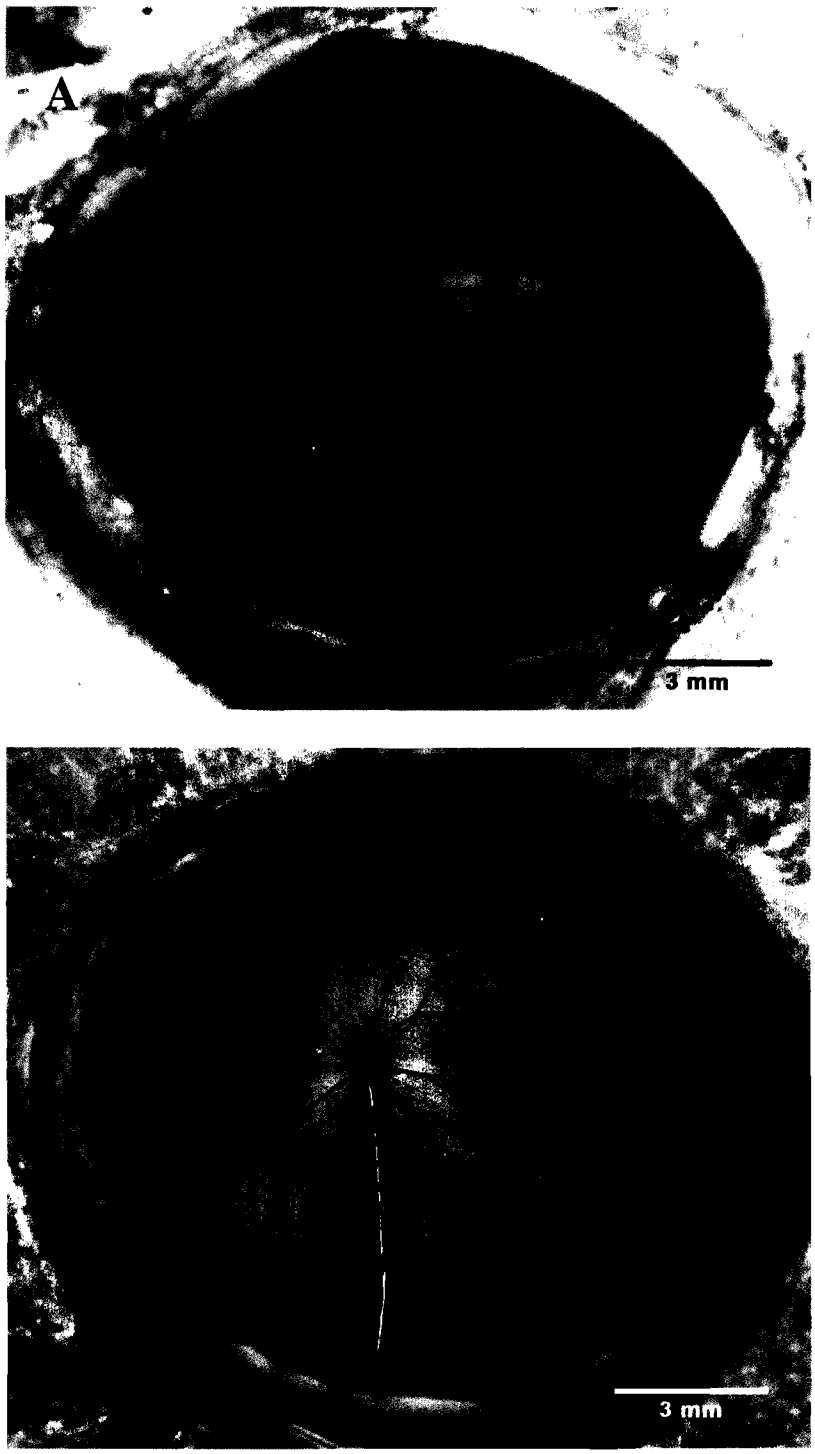

Figure 3.3. Representative digital images of the hyaloid vessels on the vitrad surface of the retina of two species of Nototheniid fishes (+Hb). (A) *Trematomus hansoni*; (B) *Notothenia coriiceps*. The cornea, iris, lens, and vitreous body were removed to allow viewing of the hyaloid vasculature. Blood vessels were traced using a digitizing tablet.

Morphometry of retinal vasculature

As a general trend, length densities of blood vessels increase as Hct decreases among Antarctic notothenioids across an approximate 2.3-fold range of Hct. Channichthyids display vessel length densities (*C. aceratus*, 5.51±0.32 mm/mm^2; *C. gunnari*, 5.15±0.50 mm/mm^2) that are similar to the observed length density in *G. acuticeps*, a red-blooded species possessing an intermediate Hct (5.20±0.46 mm/mm^2) (Table 3.2). Length densities in icefishes are greater than red-blooded species with comparatively large Hct (*P. charcoti*, 4.40±0.30 mm/mm^2; *T. hansoni*, 3.94±0.08 mm/mm^2; *N. coriiceps*, 2.48±0.21 mm/mm^2).

In addition to greater length densities, hemoglobinless (-Hb) fishes have average vessel diameters that are ~1.5 times greater than vessel diameters of +Hb species (-Hb, 0.193±0.006 mm; +Hb, 0.125±0.005 mm). The combination of greater length densities and greater vessel diameters results in significantly greater fractional image areas (percent of reference area covered by blood vessels) in icefishes than in red-blooded fishes (Table 3.2). In other words, species of fish that lack Hb have larger blood vessel surface areas available for gas exchange than +Hb fishes and have vascular capacities capable of supporting larger blood volumes than red-blooded fishes.

Fractional image area varies as a function of location on the fundus of the eye. In general, the ventrotemporal (QI) and ventronasal (QIV) regions have the greatest fractional areas, indicating that blood vessel surface area is at a maximum in the ventral region of the eye (Figure 3.4). However, *C. gunnari* does not adhere to this pattern, as fractional image areas are fairly uniform throughout all four quadrants for this species.

Table 3.2. Morphometric measurements of vascular anatomy in retinal tissues of Antarctic notothenioid fishes

	Channichthyidae		Bathydraconidae		Nototheniidae	
	Chaenocephalus aceratus (-Hb)	*Champsocephalus gunnari* (-Hb)	*Gymnodraco acuticeps* (+Hb)	*Parachaenichthyes charcoti* (+Hb)	*Trematomus hansoni* (+Hb)	*Notothenia coriiceps* (+Hb)
Length Density (mm/mm^2)	5.509 ± 0.317^{a}	$5.146 \pm 0.497^{a,b}$	$5.202 \pm 0.465^{a,b}$	$4.400 \pm 0.296^{a,b}$	3.942 ± 0.080^{b}	2.483 ± 0.214^{c}
Vessel Diameter (mm)	0.196 ± 0.009^{a}	0.186 ± 0.002^{a}	0.138 ± 0.003^{b}	0.115 ± 0.004^{c}	X	X
Fractional Image Area (%)	49.13 ± 0.98^{a}	43.75 ± 2.56^{b}	32.97 ± 2.39^{c}	23.79 ± 2.13^{d}	X	X
IVD (mm)	0.293 ± 0.016^{a}	0.308 ± 0.030^{a}	0.307 ± 0.030^{a}	0.364 ± 0.027^{a}	0.399 ± 0.008^{a}	0.646 ± 0.051^{b}
VDI (intersections/unit length)	3.507 ± 0.202^{a}	$3.276 \pm 0.316^{a,b}$	$3.312 \pm 0.296^{a,b}$	$2.801 \pm 0.188^{a,b}$	2.491 ± 0.061^{b}	1.581 ± 0.136^{c}

Length Density is the total length of vessels occupying a given area; Vessel Diameter is the width of blood vessels measured to the outside walls; VDI, Vascular Density Index; IVD, Intervessel Distance; Fractional Image Area is the percentage of reference area occupied by blood vessels.
X signifies that a measurement was not able to be obtained from that species.
Values are means ± S.E.M.; N=5 for *C. aceratus* and *P. charcoti*; N=2 for *C. gunnari*; N=3 for *G. acuticeps* and *T. hansoni*; N=4 for *N. coriiceps*.
For vessel diameter measurements, N=4 for *C. aceratus* and *P. charcoti*.
Superscripts a, b and c denote significant differences among the six species ($P \leq 0.05$).

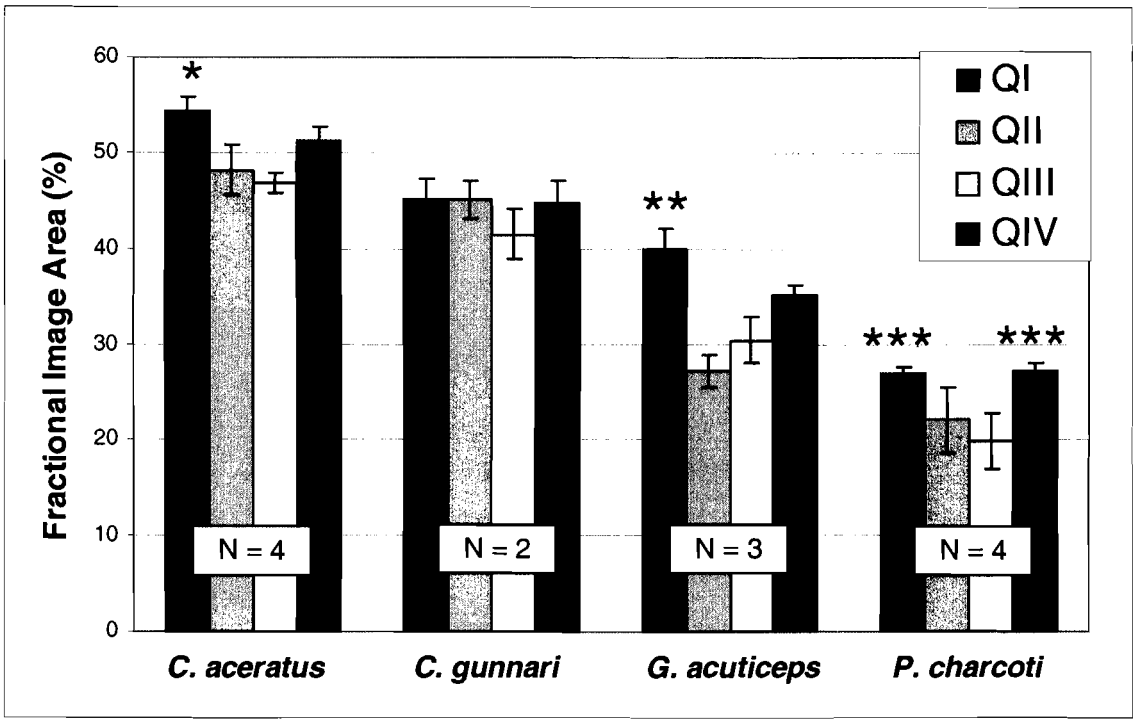

Figure 3.4. Fractional image area as a function of location on the fundus of the eye for white and red-blooded notothenioid fishes. Fractional image area is the percent of reference area covered by blood vessels. *C. aceratus* and *C. gunnari* are channichthyids; *G. acuticeps* and *P. charcoti* are red-blooded bathydraconids. QI,ventrotemporal region; QII, dorsotemporal region; QIII, dorsonasal region; QIV, ventronasal region. * denotes QI is different from QIII; ** QI is different from QII and QIII; *** QI and QIV are both different from QIII. $P \leq 0.05$ for all comparisons.

Relationships of Hct with intervessel distance and Vascular Density Index

Intervessel distance (IVD), the average path length between neighboring vessels, increases in close relation to increasing levels of Hct (Table 3.2). Among six species of white- and red-blooded notothenioids, icefishes display the smallest IVD (*C. aceratus*, 0.293±0.016 mm; *C. gunnari*, 0.308±0.030 mm), thus indicating the shortest pathways for gaseous diffusion between vessels and underlying retina (path length for gas diffusion is IVD/2). *N. coriiceps*, at the far end of the red-blooded spectrum, has the largest IVD (0.646±0.051 mm) and consequently, the longest pathways for diffusion. Among +Hb

notothenioids, IVDs in retinal tissues are positively correlated with level of Hct (Figure 3.5). Vascular Density Index (VDI) exhibits over a 50% reduction as Hct increases among +Hb fishes (Table 3.2) and most impressively, is directly related to level of Hct with a correlation coefficient of R^2=0.934 (Fig. 3.5). Red-blooded fishes show general patterns of enhanced VDI, similar to fractional image area, in ventral regions of the eye. However, differences in quadrant vascular densities are only significant in two out of four species (Figure 3.6). Quadrants I and IV in *N. coriiceps* have a distinctly greater VDI than quadrants II and III, therefore indicating the ventral region as the predominate area for vascular gas exchange. Vessel densities are also clearly dominant in the lower portion of the eye in *G. acuticeps*.

VDI and IVD may indicate regions of enhanced gas exchange

VDI and IVD were analyzed as a function of distance from the optic disc for each individual species. Locations of high VDI and low IVD are possible areas of enhanced gas exchange. Points where VDI increases and IVD decreases in conjunction are the obvious sites for transitions to areas of increased respiratory activity of the underlying tissue. However, only one species, *C. aceratus* clearly exhibits this pattern (Figure 3.7). Greatest potential for gas exchange may occur approximately 1.5-3.0 mm from the optic disc in this channichthyid species. In *P. charcoti*, *T. hansoni*, and *N. coriiceps*, VDI initially decreases and then becomes constant; conversely, IVD initially increases before becoming constant (Figures 3.8, 3.9). Predominant gas exchange in these species most likely occurs near the optic disc. VDI and IVD for *C. gunnari* and *G. acuticeps* are

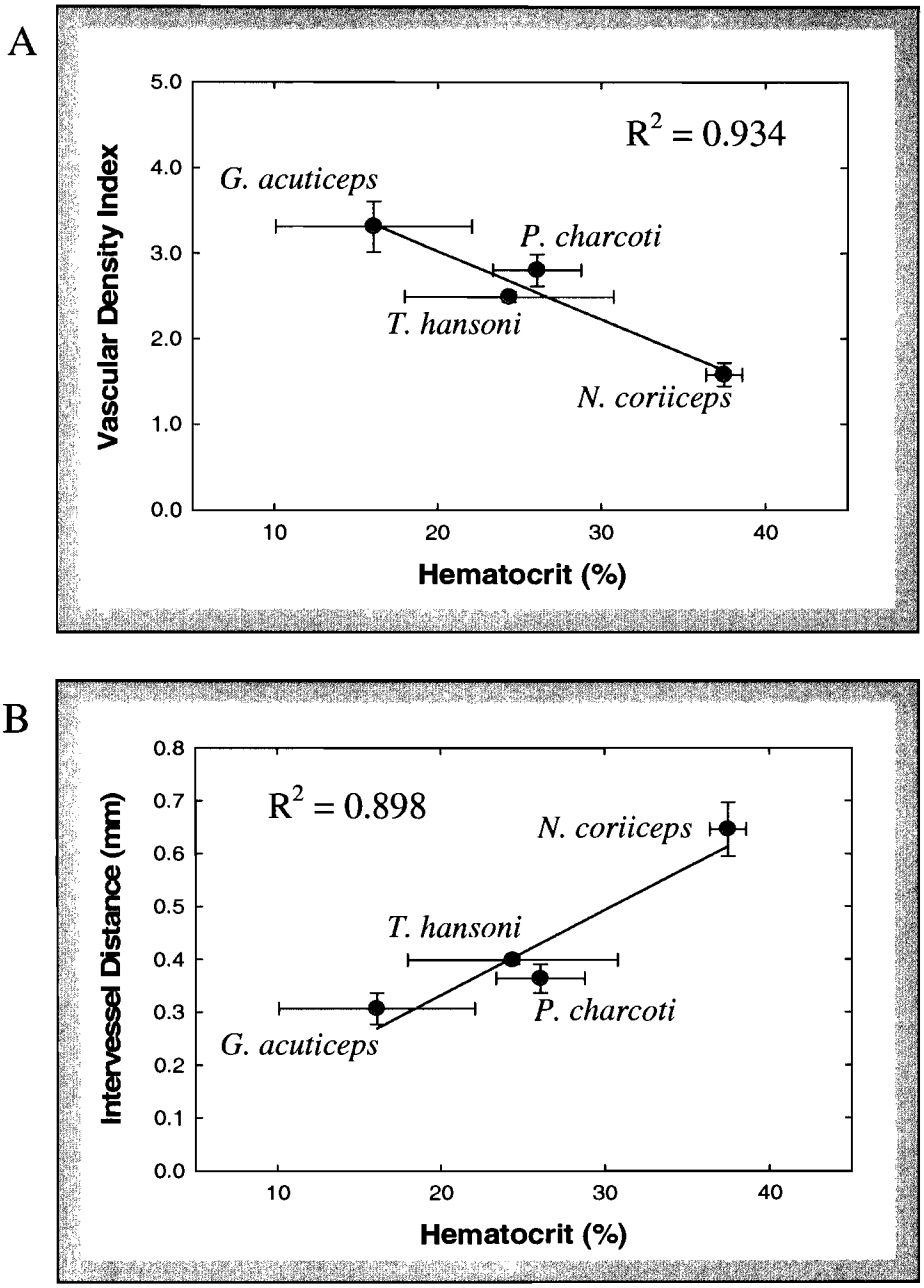

Figure 3.5. Hematocrit is related to intervessel distance and Vascular Density Index. (A) Among four red-blooded notothenioids with a >2.3-fold range of Hct, VDI in retinal tissue is inversely correlated with Hct (R^2=0.934). (B) Intervessel distance in retinal tissue, in the same four species, is positively correlated with Hct (R^2= 0.898).

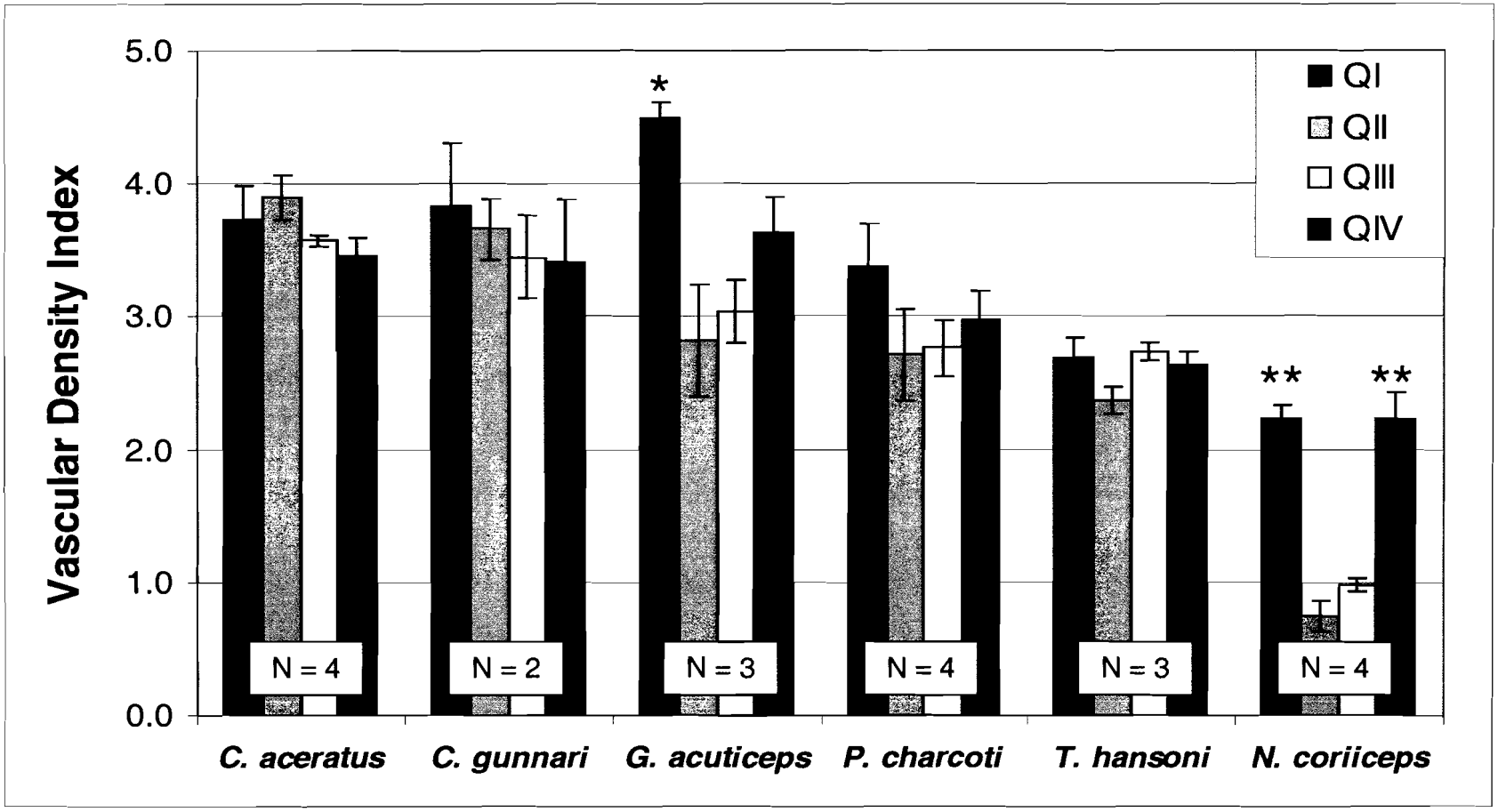

Figure 3.6. Vascular Density Index (VDI) as a function of location on the fundus of the eye for white and red-blooded notothenioid fishes. VDI is the number of vessel-grid intersections per unit length of gridline. *C. aceratus* and *C. gunnari* are channichthyids; *G. acuticeps* and *P. charcoti* are red-blooded bathydraconids; *T. hansoni* and *N. coriiceps* are red-blooded nototheniids. QI,ventrotemporal region; QII, dorsotemporal region; QIII, dorsonasal region; QIV, ventronasal region. * denotes QI is different from QII and QIII; ** QI and QIV are different from QII and QIII. $P \leq 0.05$ for all comparisons.

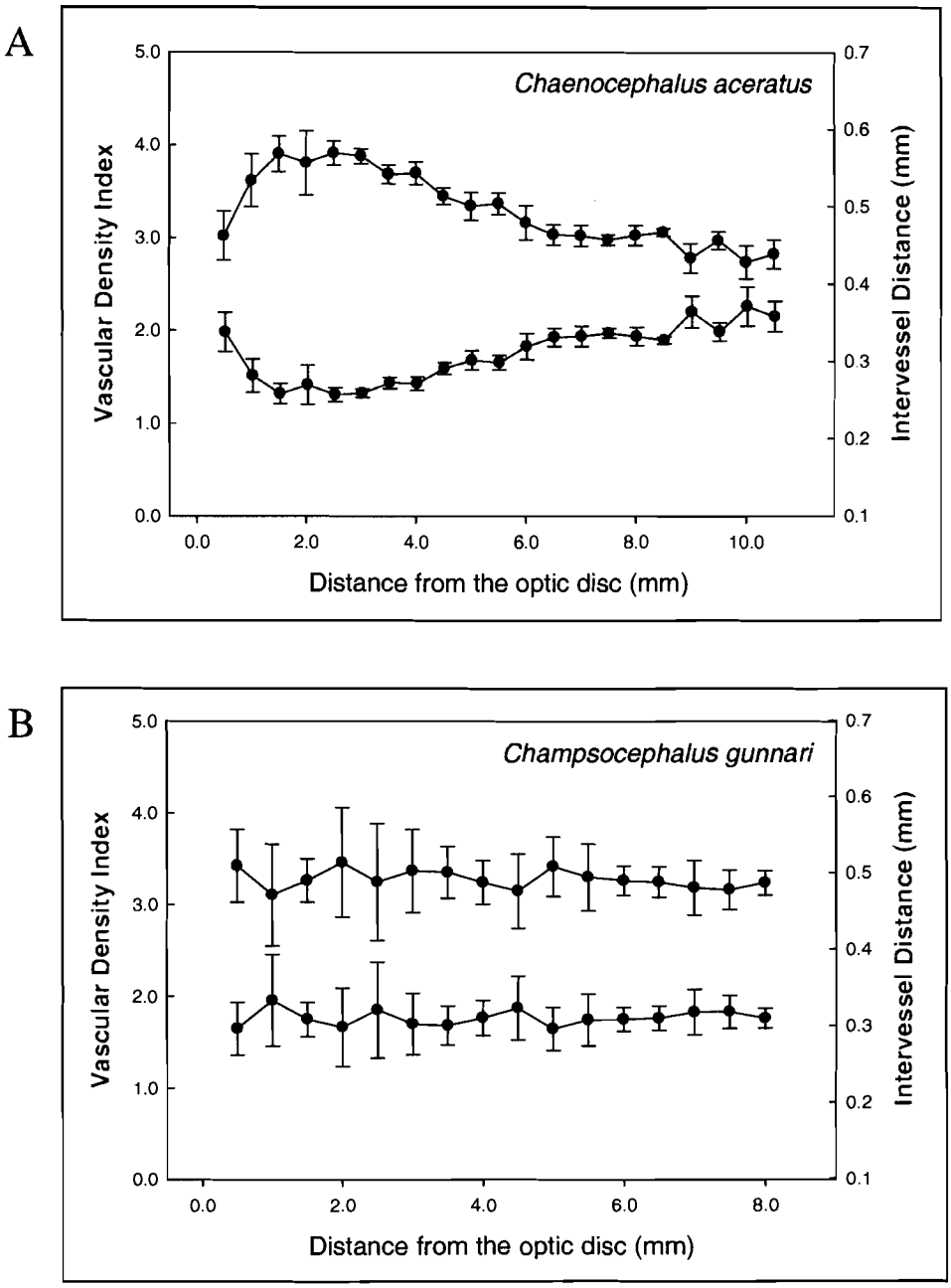

Figure 3.7. Vascular Density Index (VDI) and Intervessel Distance (IVD) as a function of distance from the optic disc for two species of channichthyid fish (-Hb). (A) *C. aceratus*, N=4; (B) *C. gunnari*, N=2.

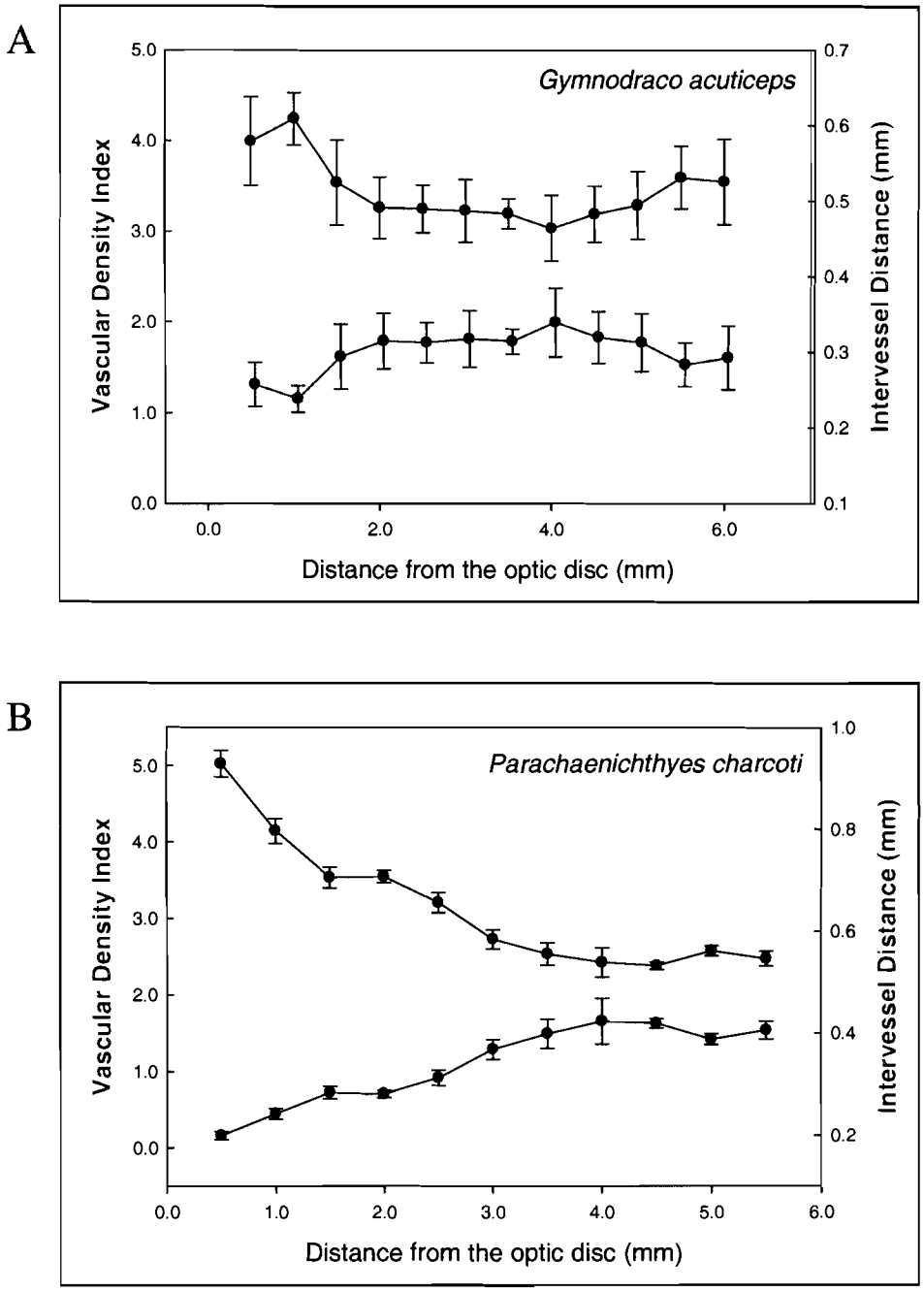

Figure 3.8. Vascular Density Index (VDI) and Intervessel Distance (IVD) as a function of distance from the optic disc for two species of bathydraconid fish (+Hb). (A) *G. acuticeps*, N=3; (B) *P. charcoti*, N=4.

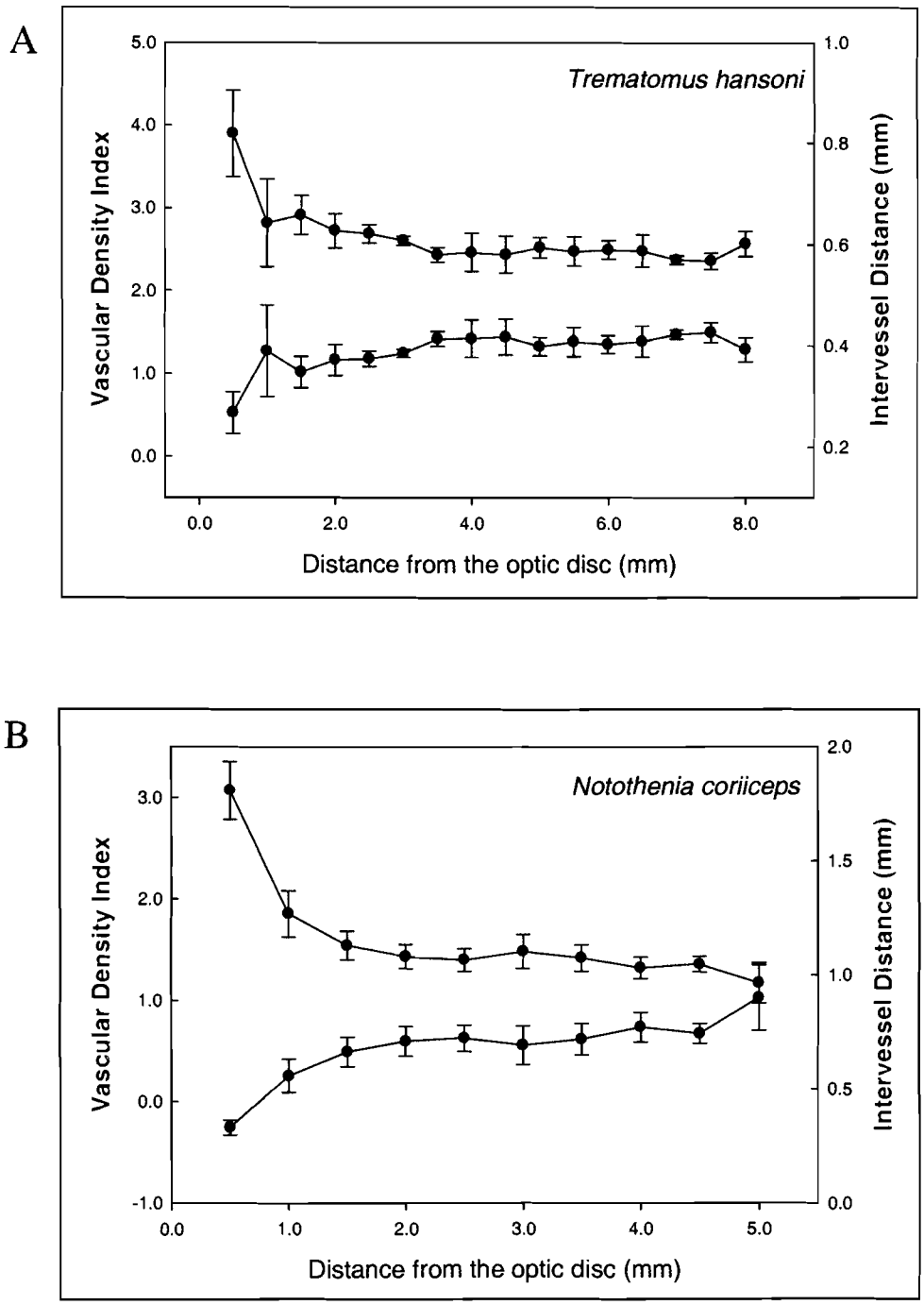

Figure 3.9. Vascular Density Index (VDI) and Intervessel Distance (IVD) as a function of distance from the optic disc for two species of nototheniid fish (+Hb). (A) *T. hansoni*, N=3; (B) *N. coriiceps*, N=4.

nearly uniform for the majority of the eye, indicating that gaseous exchange in these species may change little as a function of distance from the optic disc (Figures 3.7, 3.8).

Measurement variability associated with MATLAB macro

Intra-observer variability associated with use of the MATLAB macro developed for this research was <1% for each species analyzed. Among +Hb fishes, variability decreased in relation to decreasing complexity of the vascular pattern. The 0% variability for *N. coriiceps* indicates the highest degree possible for data reproduction, although all intra-observer variability data certainly fall within acceptable limits (Table 3.3).

Table 3.3. Measurement variability associated with use of MATLAB macro developed for this study

	C.aceratus (-Hb)	*C. gunnari* (-Hb)	*G. acuticeps* (+Hb)	*P. charcoti* (+Hb)	*T. hansoni* (+Hb)	*N. coriiceps* (+Hb)
Intra-Observer Variability (%)	0.34	0.37	0.96	0.64	0.14	0.00

Chapter 4

Discussion

Retinal tissue is highly aerobic and requires considerable oxygen to sustain normal physiological function (Wittenberg and Wittenberg, 1974). The morphometric characterization presented here begins to explain how adequate oxygen tensions are maintained in the eyes of notothenioid fishes despite decreases in the levels of or, in some cases, the complete lack of circulating erythrocytes containing hemoglobin. Dramatic differences in geometries of ocular vessels exist between white- (-Hb) and red-blooded (+Hb) Antarctic fishes. More subtle variations in pattern are displayed among +Hb species with differing Hcts. The quantitative description of the vasculature on the vitrad surface of the retina presented in this study substantiates previous qualitative accounts (Eastman, 1988; Eastman and Lannoo, 2004; Sidell and O'Brien, 2006). With the exception of vessel diameters, other quantitative data describing morphometry of blood vessels associated with the retina of the eye of notothenioid fishes are lacking.

Manual point-counting methods have traditionally been used to quantify biological structures (Weibel, 1979) but, in recent years, it has become more common to employ digital systems for morphometric analyses (Abrams et al., 1994; Rieder et al., 1995). Automated image analysis decreases processing time and includes methods that are highly reproducible. This study described an originally developed MATLAB macro that generated intra-observer variability values of <1% for all species sampled. This is an improvement over previous measurement variability for automated image analysis systems (Maas et al., 1999; Voss et al., 1984). It is therefore a highly efficient method

with which to quantify vascular arrays in the eye. This method may be suited to many other applications, particularly for quantification of biological structures arranged radially around a central point.

Vascular geometries in retinal tissues differ among –Hb and +Hb fishes

Average length densities of vessels in retinas from -Hb channichthyids (5.33±0.41 mm/mm^2) vary little from mean densities in +Hb bathydraconids that possess intermediate Hct (4.80±0.39 mm/mm^2), but are ~1.5 times greater than mean length densities observed in +Hb nototheniids possessing comparatively large Hct (3.21±0.15 mm/mm^2). Surprisingly, this observation contrasts with the relationship observed in pectoral muscle for -Hb *C. aceratus* and +Hb *N. coriiceps*, where length densities in both species are relatively similar (*C. aceratus*, 880±73 mm^{-2}; *N. coriiceps,* 1057±114 mm^{-2}) (O'Brien et al., 2003). Mean capillary cross-sectional area in skeletal muscle of *C. aceratus* is ~1.6 times greater than in *N. coriiceps* (O'Brien et al., 2003) and 2-3 times greater than recorded values in most other red-blooded teleosts (Fitch et al., 1984). Supporting these data, mean vessel diameters in retinal tissue of white-blooded channichthyids in this study are ~1.5 times greater than those of red-blooded bathydraconids. Due to problems with the Microfil™ preparations for higher Hct nototheniids, vessel diameters from these species are not available for comparison.

Increases in vessel diameter reduce peripheral resistance to blood flow. Poiseuille's Equation shows that relatively small increases in vessel diameter result in large increases in flow:

$$Q = [(P_1 - P_2)\, \pi r^4 / 8L\eta]$$

where Q, the flow rate of the fluid (blood), is directly proportional to the pressure difference $P_1 - P_2$ along the length of the vessel, and the fourth power of the radius of the vessel, r. Flow rate is inversely proportional to the length of the vessel, L, and fluid viscosity, η. Viscosity of fluids is inversely proportional to temperature. A decrease in hematocrit reduces blood viscosity and helps to offset the effect of depressed temperature, thereby enhancing blood flow (Egginton, 1996; Hemmingsen and Douglas, 1972; Wells et al., 1990). Ultimately, high flow rates facilitate large vessel-tissue Po_2 gradients along the length of the vascular bed, leading to greater diffusive fluxes of oxygen between vessels and retina.

Vessel densities found in retinal tissues of -Hb species and +Hb species possessing low Hct are enhanced compared to densities in +Hb fishes with higher Hct. Increased vessel densities not only reduce peripheral resistance, but also decrease the mean diffusion path length for oxygen, resulting in a greater rate of oxygen delivery to retinal tissue. In combination with cardiovascular modifications (large diameter vessels, blood volumes, hearts, and cardiac outputs), Hb-deficient notothenioids maintain normal biological function in the eye by compensations that include high densities of large-bore vessels and short path lengths for oxygen diffusion. Red-blooded Antarctic fishes, with modest vessel diameters compensate for reduced Hb mainly by increasing the number of ocular vessels and, consequently, shortening oxygen-diffusion distances between vessels and underlying retina.

Vascular geometries vary with location on the fundus of the eye

Antarctic notothenioids display a more extensive and homogeneous pattern of hyaloid vessels compared to the majority of teleosts studied to date (Anctil, 1968; Eastman, 1988; Hanyu, 1962). Eastman (1988) described the notothenioid hyaloid pattern as being radially asymmetrical, with slightly greater densities on the ventral and nasal fields. He observed no marked differences in vessel distribution between central and peripheral regions of the retina. This is unlike the remarkable pattern seen in the cyprinodontid *Fundulus grandis*, where a highly vascularized area centralis is observed ventral to the optic disc (Copeland, 1976). Vascular geometries of notothenioids examined here generally conform to the above qualitative characterization by Eastman. Indeed, densities are greater on the ventral aspect of the retina. At the same time, quantitative analyses revealed a slightly higher density of vessels in the temporal field than in the nasal field of the retina. Quantitative methods also detected a region of high vascular density and low intervessel distance within the hyaloid vasculature of *C. aceratus* within the first 30% of the fundus as a function of distance from the optic disc. This region identified in *C. aceratus* may represent a more vascularized area centralis, similar to that of *F. grandis*.

Hematocrits are correlated to vascular geometries

Hematocrit was used as a proxy for hemoglobin concentration, an assumption that needs verification. Hb concentrations among red-blooded fishes vary in a manner similar to Hct, but not necessarily with the same magnitude between each species (Egginton, 1994; Kooyman, 1963; Kunzmann, 1991). Utilizing published Hb data (Table 4.1), a

strong linear relationship between Hb concentration and vascular densities is observed for three red-blooded species ($R^2 = 0.98$ for correlation between VDI and Hb; $R^2 = 0.88$ for correlation between VDI and Hct). Hb content is directly related to vascular densities among +Hb notothenioids and the relationship between them is similar to the relationship observed between Hct and vascular densities, thus validating the use of Hct as a proxy for Hb concentration.

Table 4.1. Vascular densities and hematologic parameters of +Hb notothenioid fishes

Species	N	VDI	Hct (%)	Hb (g/L)	Data Source
G. acuticeps	≥10	3.31	14	20.1	Kunzmann 1991
T. hansoni	8	2.49	29	28	Kooyman 1963
N. coriiceps	5	1.58	33	60.4	Egginton 1994

N = sample size; VDI = Vascular Density Index; Hct = hematocrit; Hb = hemoglobin content.
Sample size corresponds to Hct and Hb data.
VDI data are values from the present study.
Hct and Hb data from listed sources reflect values similar to data obtained in the present study.

Enhanced blood flow enables hemoglobinless icefishes to achieve sufficient oxygen tension in retinal tissues with fewer vessels than would be expected by extrapolation of the relationship between vascular density and Hct observed in red-blooded notothenioids (Fig. 5). Unfortunately, lack of data pertaining to blood circulation in +Hb fishes from this study makes it difficult to assess systemic effects on retinal vasculature among these species. Axelsson and associates (1992) reported cardiovascular indices for two red-blooded nototheniids, *Pagothenia bernacchii* (benthic) and *Pagothenia borchgrevinki* (cryopelagic), that occupy different ecological niches. Hct of *P. borchgrevinki*, an active species, is ~1.5 times greater than the sedentary *P.*

bernacchii (Eastman, 1993). Cardiac outputs, heart rates, stroke volumes, ventral aortic pressures, and total vascular resistances did not differ between the two species (Axelsson et al., 1992). Species of red-blooded notothenioids from the present study are benthic fishes, while activity levels vary among them (Eastman, 1993). Given the natural histories of the red-blooded fishes in the present study it is likely that blood flows are not drastically different among them. A growing body of research on cardiovascular indices (i.e., cardiac outputs, heart rates, stroke volumes, etc.) of blood flows suggests that systemic circulations in white-blooded notothenioids are very different from those of red-blooded fishes (Axelsson et al., 1992; Hemmingsen et al., 1972; Holeton, 1970). Because of the uncontrolled mitigating effect of differences in blood flow, channichthyids were not included in the regression analysis relating Hct to anatomical vascular characteristics.

One additional factor in the eye may influence the number of vessels on the vitrad surface of the retina. A choroid rete, a horseshoe-shaped structure consisting of arterial and venous capillaries in parallel array, is found in some species at the back of the eye around the optic nerve (Eastman, 1993). Using countercurrent multiplication, the rete generates elevated oxygen tensions in the choroid, a layer of the eye just posterior to the sclerad surface of the retina and near the photoreceptors (Wittenberg and Wittenberg, 1974). The rete is present in most species of Nototheniidae but is lost in more phyletically derived families, Channichthyidae and Bathydraconidae (Eastman, 1993). Recently, however, it was discovered that one bathydraconid, *P. charcoti*, possesses microscopic retia (Eastman and Lannoo, 2003). If oxygen tensions are elevated to high enough levels on the sclerad surface of the retina, diffusive flux may be sufficient to

supply the majority of the retina with oxygen, and fewer vessels would be necessary on the vitrad surface. In other words, possession of a choroid rete could directly relate to vascular densities. The results reported in this study reveal no obvious correlation between presence/absence of the rete and vascular density of the retina. For instance, *N. coriiceps* and *T. hansoni* both possess retes, yet each species exhibits significantly different vascular densities. Consequently, it appears that the relationship between Hct and vascular densities is unaffected by possession of a choroid rete.

Vascular densities may reflect NO-mediated angiogenesis

NO could be an intermediary between Hct and vascular densities in notothenioids. The presence of NOS has been established in various tissues from different species of teleosts. In ocular tissues, eNOS is localized to Müller cells and axon terminals of horizontal cells in the retina of white bass (Haverkamp et al., 1999). Fritsche and colleagues (2000) demonstrated NOS immunoreactivity in endothelial cells of the dorsal vein and in the heart of larval zebrafish and found that vasculature was influenced by endogenously produced NO. Their study provided evidence that vascular tone in larval tissues is regulated by local production of NO before functional autonomic innervation of the peripheral vascular system occurs (Fritsche et al., 2000). There is no existing data on the expression of NOS or concentrations of NO in the eyes of notothenioids. However, NOS has been noted in the heart and branchial vasculature of icefishes (Pellegrino et al., 2003) and Morla et al. (2003) demonstrated that -Hb channichthyids express higher levels of nNOS in skeletal muscle compared to +Hb notothenioids. In addition, preliminary data from our laboratory suggests that circulating levels of NO in channichthyids are >2-

fold those observed in red-blooded notothenioids (Sidell and O'Brien, 2006). Research to date indicates a role for NO in teleosts and also supports the assumption that NO concentration is related to Hct in Antarctic fishes.

In skeletal muscles of mammals, primary molecular responses to limited oxygen availability are upregulation of NOS and subsequent increases in NO synthesis. This leads to vasodilation of vessels and concomitant increases of blood flow (Lau et al., 2000). Secondary responses are activation of hypoxia-inducible factor alpha (HIF-α) and induction of expression of vascular endothelial growth factor (VEGF), which stimulates angiogenesis in muscles (Ikeda et al., 1995; Wagner, 2001). Morla et al. (2003) concluded that high expression of nNOS in muscles of icefishes was a molecular compensation for lack of Hb, even though expression of VEGF in icefishes was similar to expression in red-blooded species. This indicates that expression of nNOS in muscles of icefishes may lead to a primary vasodilatory response and not the secondary response of angiogenesis. This is consistent with the findings of O'Brien (2003); she found no differences between the vascular length densities in pectoral muscles of red- and white-blooded notothenioids, but capillary cross-sectional areas were greater in white-blooded species.

Prolonged imbalances between oxygen delivering capacities of blood vessels and metabolic demands of tissues may lead to modification of the vasculature to satisfy the needs of the tissue (Adair et al., 1990). Metabolic supply and demand in muscles of notothenioids is different from that of retinal tissue. Increased levels of nNOS in muscle may stimulate vasodilation, rather than angiogenesis, thereby enhancing blood flow to the tissue (Morla et al., 2003). An exclusive vasodilatory response might be sufficient to

meet the metabolic needs of muscle tissue and adding vessels to further increase oxygen delivering capacity would be unnecessary. In the eye, vasodilation alone may not be enough to increase oxygen delivering capacity to meet the high metabolic demands of the retina. This would, therefore, necessitate a greater number of vessels to aid oxygen transport to retinal cells. Enhanced vessel densities in retinal tissues of -Hb icefishes may indicate a secondary molecular response of angiogenesis as compensation for lack of Hb and high metabolic demand of retinal cells.

Angiogenic response appears to be a tissue-specific phenomenon in notothenioids. With limited data to draw upon, one can only speculate as to the possible explanation for this enigma. One answer might be the involvement of homeostatic feedback mechanisms. At some point, metabolic demands of a tissue will be satisfied. When that occurs, such as in muscle tissues of white-blooded notothenioids, it is plausible that a molecular signal(s) halts the vasodilatory response and prevents further enhancement of blood flow by blocking the angiogenic pathway. In terms of energetics, this is a reasonable explanation because it would not make sense to continue to expend energy in restructuring the vasculature if metabolic requirements have already been fulfilled. Even in systems without increased steady-state levels of NO, one would expect a mechanism to be in place under normal physiological conditions to counteract an upregulating pathway. As the possibilities are manifold, this will likely remain an unresolved issue until more is known about NO activities in notothenioids.

Concluding remarks

White-blooded icefishes possess retinal vascular anatomies that are characterized by elevated densities of large-bore vessels spaced short distances apart. This reduces path lengths for gas exchange and promotes diffusion of oxygen between vessels and retina. Red-blooded notothenioids display retinal vascular geometries that vary in direct relation to the amount of Hb they possess. Thus, notothenioid species with reduced Hb concentrations have denser patterns with slightly larger diameter vessels than species possessing larger Hb contents. Enhanced vascular densities of Hb-deficient fishes suggest that angiogenesis may have occurred in retinal tissue to compensate oxygen delivering capacity to this highly aerobic tissue. NO is known to stimulate vascular proliferation and is an obvious candidate as possible intermediary between Hb concentration and vascular density. Substantiating this association, recent evidence indicates that NO levels are greater in -Hb fishes compared to +Hb species. Therefore, vascular densities in retinal tissues of Hb deficient Antarctic fishes may reflect NO-mediated angiogenesis.

REFERENCES

Abrams, D. C., Facer, P., Bishop, A. E. and Polak, J. M. (1994). A computer-assisted stereological quantification program: OpenStereo. *Microsc Res Tech* 29, 240-7.

Adair, T. H., Gay, W. J. and Montani, J. P. (1990). Growth regulation of the vascular system: evidence for a metabolic hypothesis. *Am J Physiol* 259, R393-404.

Anctil, M. (1968). Intraocular vascular supply in some marine teleosts. *Rev Can Biol* 27, 347-355.

Axelsson, M., Davison, W., Forster, M. E. and Farrell, A. P. (1992). Cardiovascular responses of the red-blooded Antarctic fishes Pagothenia bernacchii and P. borchgrevinki. *J Exp Biol* 167, 179-201.

Chase, J. (1982). The evolution of retinal vascularization in mammals. A comparison of vascular and avascular retinae. *Ophthalmology* 89, 1518-25.

Conway, E. M., Collen, D. and Carmeliet, P. (2001). Molecular mechanisms of blood vessel growth. *Cardiovasc Res* 49, 507-21.

Copeland, D. E. (1976). The anatomy and fine structure of the eye in teleost. IV. The choriocapillaris and the dual vascularization of the area centralis in *Fundulus grandis*. *Exp Eye Res* 22, 169-179.

Eastman, J. T. (1988). Ocular Morphology in Antarctic Notothenioid Fishes. *J Morphol* 196, 283-306.

Eastman, J. T. (1993). Antarctic Fish Biology: Evolution in a Unique Environment. San Diego: Academic Press.

Eastman, J. T. and Eakin, R. R. (2000). An updated species list for notothenioid fish (Perciformes; Notothenioiei), with comments on Antarctic species. *Arch Fish Mar Res* 48, 11-20.

Eastman, J. T. and Lannoo, M. J. (2003). Diversification of brain and sense organ morphology in Antarctic dragonfishes (Perciformes: Notothenioidei: Bathydraconidae). *J Morphol* 258, 130-50.

Eastman, J. T. and Lannoo, M. J. (2004). Brain and sense organ anatomy and histology in hemoglobinless Antarctic icefishes (Perciformes: Notothenioidei: Channichthyidae). *J Morphol* 260, 117-40.

Egginton, S. (1994). Stress response in two Antarctic teleosts (*Notothenia coriiceps* Richardson and *Chaenocephalus aceratus* Lonnberg) following capture and surgery. *J Comp Physiol B* 164, 482-491.

Egginton, S. (1996). Blood rheology of Antarctic fishes: viscosity adaptations at very low temperatures. *J Fish Biol* 48, 513-521.

Fitch, N. A., Johnston, I. A. and Wood, R. E. (1984). Skeletal muscle capillary supply in a fish that lacks respiratory pigments. *Respir Physiol* 57, 201-211.

Fritsche, R., Schwerte, T. and Pelster, B. (2000). Nitric oxide and vascular reactivity in developing zebrafish, Danio rerio. *Am J Physiol Regul Integr Comp Physiol* 279, R2200-7.

Gardner, P. R. (2005). Nitric oxide dioxygenase function and mechanism of flavohemoglobin, hemoglobin, myoglobin and their associated reductases. *J Inorg Biochem* 99, 247-66.

Gon, O. and Heemstra, P. C. (1990). Fishes of the Southern Ocean, pp. 462. Grahamstown: J. L. B. Smith Institute of Ichthyology.

Hanyu, I. (1962). Intraocular vascularization in some fishes. *Can J Zool* 40, 87-106.

Haverkamp, S., Kolb, H. and Cuenca, N. (1999). Endothelial nitric oxide synthase (eNOS) is localized to Muller cells in all vertebrate retinas. *Vision Res* 39, 2299-303.

Hemmingsen, E. A. (1991). Respiratory and cardiovascular adaptations in hemoglobin-free fish: resolved and unresolved problems. In *Biology of Antarctic Fish*, eds. G. di Prisco B. Maresca and B. Tota), pp. 191-203. New York: Springer-Verlag.

Hemmingsen, E. A. and Douglas, E. L. (1970). Respiratory characteristics of the hemoglobin-free fish Chaenocephalus aceratus. *Comp Biochem Physiol* 33, 733-44.

Hemmingsen, E. A. and Douglas, E. L. (1972). Respiratory and circulatory responses in a hemoglobin-free fish, Chaenocepahlus aceratus, to changes in temperature and oxygen tension. *Comp Biochem Physiol A* 43, 1031-43.

Hemmingsen, E. A., Douglas, E. L., Johansen, K. and Millard, R. W. (1972). Aortic blood flow and cardiac output in the hemoglobin-free fish Chaenocephalus aceratus. *Comp Biochem Physiol A* 43, 1045-51.

Holeton, G. F. (1970). Oxygen uptake and circulation by a hemoglobinless Antarctic fish (Chaenocephalus aceratus lonnberg) compared with three red-blooded Antartic fish. *Comp Biochem Physiol* 34, 457-71.

Holmqvist, B., Ellingsen, B., Forsell, J., Zhdanova, I. and Alm, P. (2004). The early ontogeny of neuronal nitric oxide synthase systems in the zebrafish. *J Exp Biol* 207, 923-35.

Ikeda, E., Achen, M. G., Breier, G. and Risau, W. (1995). Hypoxia-induced transcriptional activation and increased mRNA stability of vascular endothelial growth factor in C6 glioma cells. *J Biol Chem* 270, 19761-6.

Kerwin, J. F., Jr., Lancaster, J. R., Jr. and Feldman, P. L. (1995). Nitric oxide: a new paradigm for second messengers. *J Med Chem* 38, 4343-62.

Kimura, H., Weisz, A., Kurashima, Y., Hashimoto, K., Ogura, T., D'Acquisto, F., Addeo, R., Makuuchi, M. and Esumi, H. (2000). Hypoxia response element of the human vascular endothelial growth factor gene mediates transcriptional regulation by nitric oxide: control of hypoxia-inducible factor-1 activity by nitric oxide. *Blood* 95, 189-97.

Knox, G. A. (1970). Antarctic marine ecosystems. In *Antarctic Ecology*, vol. 1 (ed. M. W. Holdgate), pp. 69-96. London: Academic Press.

Kooyman, G. L. (1963). Erythrocyte analysis of some Antarctic fishes. *Copeia* 2, 457-458.

Kunzmann, A. (1991). Blood physiology and ecological consequences in Weddell Sea fishes (Antarctica). *Ber Polarforsch* 91, 1-79.

Lau, K. S., Grange, R. W., Isotani, E., Sarelius, I. H., Kamm, K. E., Huang, P. L. and Stull, J. T. (2000). nNOS and eNOS modulate cGMP formation and vascular response in contracting fast-twitch skeletal muscle. *Physiol Genomics* 2, 21-7.

Laws, R. M. (1985). The ecology of the Southern Ocean. *Am Sci* 73, 26-40.

Lewis, R. W. and Perkin, R. G. (1985). The winter oceanography of McMurdo Sound, Antarctica. In *Antarctic Research Series, Vol. 43, Oceanology of the Antarctic Continental Shelf*, vol. 43 (ed. S. S. Jacobs), pp. 145-165. Washington: American Geophysical Union.

Littlepage, J. L. (1965). Oceanographic investigations in McMurdo Sound, Antarctica. In *Antarctic Research Series, Vol. 5, Biology of the Antarctic Seas II*, (ed. G. A. Llano), pp. 1-37. Washington: American Geophysical Union.

Maas, J. W., Le Noble, F. A., Dunselman, G. A., de Goeij, A. F., Struyker Boudier, H. A. and Evers, J. L. (1999). The chick embryo chorioallantoic membrane as a model to investigate the angiogenic properties of human endometrium. *Gynecol Obstet Invest* 48, 108-12.

Milkiewicz, M., Hudlicka, O., Brown, M. D. and Silgram, H. (2005). Nitric oxide, VEGF, and VEGFR-2: interactions in activity-induced angiogenesis in rat skeletal muscle. *Am J Physiol Heart Circ Physiol* 289, H336-43.

Moncada, S. (1997). Nitric oxide in the vasculature: physiology and pathophysiology. *Ann N Y Acad Sci* 811, 60-7; discussion 67-9.

Moncada, S. and Higgs, A. (1993). The L-arginine-nitric oxide pathway. *N Engl J Med* 329, 2002-12.

Morla, M., Agusti, A. G. N., Rahman, I., Motterlini, R., Saus, C., Morales-Nin, B., Company, J. B. and Busquets, X. (2003). Nitric oxide synthase type I (nNOS), vascular endothelial growth factor (VEGF) and myoglobin-like expression in skeletal muscle of Antarctic icefishes (Notothenioidei: Channichthyidae). *Polar Biol* 26, 458-462.

O'Brien, K. M., Skilbeck, C., Sidell, B. D. and Egginton, S. (2003). Muscle fine structure may maintain the function of oxidative fibres in haemoglobinless Antarctic fishes. *J Exp Biol* 206, 411-421.

Palmer, R. M., Ferrige, A. G. and Moncada, S. (1987). Nitric oxide release accounts for the biological activity of endothelium-derived relaxing factor. *Nature* 327, 524-6.

Pellegrino, D., Acierno, R. and Tota, B. (2003). Control of cardiovascular function in the icefish Chionodraco hamatus: involvement of serotonin and nitric oxide. *Comp Biochem Physiol A Mol Integr Physiol* 134, 471-80.

Rieder, M. J., O'Drobinak, D. M. and Greene, A. S. (1995). A computerized method for determination of microvascular density. *Microvasc Res* 49, 180-9.

Rivkin, R. B. and Putt, M. (1987). Diel periodicity of photosynthesis in polar phytoplankton: Influence on primary production. *Science* 238, 1285-1288.

Ruud, J. T. (1954). Vertebrates without erythrocytes and blood pigment. *Nature* 173, 848-850.

Sidell, B. D. and O'Brien, K. M. (2006). When bad things happen to good fish: the loss of hemoglobin and myoglobin expression in Antarctic icefishes. *J Exp Biol* 209, 1791-1802.

Strick, D. M., Waycaster, R. L., Montani, J. P., Gay, W. J. and Adair, T. H. (1991). Morphometric measurements of chorioallantoic membrane vascularity: effects of hypoxia and hyperoxia. *Am J Physiol* 260, H1385-9.

Sullivan, C. W., Palmisano, A. C. and SooHoo, J. B. (1984). Influence of sea ice and sea ice biota on downwelling irradince and spectral composition of light in McMurdo Sound. In *Proceedings of the SPIE-The International Society for Optical Engineering*, vol. 489, Ocean Optics VII (ed. M. A. Blizard), pp. 159-165. Washington: SPIE-The International Society for Optical Engineering, Bellingham.

Suri, C., McClain, J., Thurston, G., McDonald, D. M., Zhou, H., Oldmixon, E. H., Sato, T. N. and Yancopoulos, G. D. (1998). Increased vascularization in mice overexpressing angiopoietin-1. *Science* 282, 468-71.

Tota, B., Amelio, D., Pellegrino, D., Ip, Y. K. and Cerra, M. C. (2005). NO modulation of myocardial performance in fish hearts. *Comp Biochem Physiol A Mol Integr Physiol* 142, 164-77.

Voss, K., Jacob, W. and Roth, K. (1984). A new image analysis method for the quantification of neovascularization. *Exp Pathol* 26, 155-161.

Wagner, P. D. (2001). Skeletal muscle angiogenesis. A possible role for hypoxia. *Adv Exp Med Biol* 502, 21-38.

Walls, G. L. (1942). The Vertebrate Eye and its Adaptive Radiation. Bloomfield Hills, Michigan: Cranbrook Institute of Science, Bulletin No. 19.

Weibel, E. R. (1979). Stereological Methods: Practical Methods for Biological Morphometry, Vol. 1. New York: Academic Press.

Wells, R. M. G., Ashby, M. D., Duncan, S. J. and Macdonald, J. A. (1980). Comparative study of the erythrocytes and haemoglobins in nototheniid fishes from Antarctica. *J Fish Biol* 17, 517-527.

Wells, R. M. G., Macdonald, J. A. and DiPrisco, G. (1990). Thin-blooded Antarctic fishes: a rheological comparison of the haemoglobin-free icefishes *Chionodraco kathleenae* and *Cryodraco antarcticus* with a red-blooded notothniid, *Pagothenia bernacchii*. *J Fish Biol* 36, 595-609.

Wittenberg, J. B. and Wittenberg, B. A. (1974). The choroid rete mirabile of the fish eye. I. Oxygen secretion and structure: comparison with the swimbladder rete mirabile. *Biol Bull* 146, 116-36.

BIOGRAPHY OF THE AUTHOR

Jody M. Wujcik was born in Lehighton, Pennsylvania on August 4, 1974. She was raised in Effort, Pennsylvania and graduated from Pleasant Valley High School in 1992. Jody earned Bachelor of Science degrees in Biology and Marine Science from East Stroudsburg University in 2004. She entered the Marine Biology graduate program at The University of Maine in the summer of 2004 under the guidance of Dr. Bruce D. Sidell. Jody is an associate member of the Sigma Xi Scientific Research Society.

After receiving her degree, Jody will continue to pursue her interests in comparative physiology by enrolling in the Marine Biology doctoral program at The University of Maine. Jody is a candidate for the Master of Science degree in Marine Biology from The University of Maine in August, 2006.